Normalizing translation through 4E-BP prevents mTOR-driven cortical mislamination and ameliorates aberrant neuron integration

Tiffany V. Lin[a,b], Lawrence Hsieh[a,b], Tomoki Kimura[a,b], Taylor J. Malone[a,b], and Angélique Bordey[a,b,1]

[a]Department of Neurosurgery, Yale University School of Medicine, New Haven, CT 06520; and [b]Department of Cellular and Molecular Physiology, Yale University School of Medicine, New Haven, CT 06520

Edited by Nicholas Spitzer, University of California, San Diego, La Jolla, CA, and approved August 8, 2016 (received for review April 12, 2016)

Hyperactive mammalian target of rapamycin complex 1 (mTORC1) is a shared molecular hallmark in several neurodevelopmental disorders characterized by abnormal brain cytoarchitecture. The mechanisms downstream of mTORC1 that are responsible for these defects remain unclear. We show that focally increasing mTORC1 activity during late corticogenesis leads to ectopic placement of upper-layer cortical neurons that does not require altered signaling in radial glia and is accompanied by changes in layer-specific molecular identity. Importantly, we found that decreasing cap-dependent translation by expressing a constitutively active mutant of the translational repressor eukaryotic initiation factor 4E-binding protein 1 (4E-BP1) prevents neuronal misplacement and soma enlargement, while partially rescuing dendritic hypertrophy induced by hyperactive mTORC1. Furthermore, overactivation of translation alone through knockdown of 4E-BP2 was sufficient to induce neuronal misplacement. These data show that many aspects of abnormal brain cytoarchitecture can be prevented by manipulating a single intracellular process downstream of mTORC1, cap-dependent translation.

mTOR | autism | spine | dendrite | cortical development

Overactive mammalian target of rapamycin complex 1 (mTORC1) signaling is a signature of many disorders with cortical malformations (1), ranging from tuberous sclerosis complex with focal dysplasias to hemimegalencephaly with more diffuse, hemispheric aberrations. The high incidence of negative outcomes in individuals with such malformations (2), which are often associated with intractable childhood seizures, underscores the need to better understand the molecular etiology of these developmental lesions. Animal models have demonstrated the causative effect of increased mTORC1 signaling on mislamination (3–7). The pharmacological mTORC1 blocker rapamycin has also been shown to reverse some of the developmental abnormalities and associated seizure activity in several of these mouse models (5, 6, 8–10), further emphasizing the importance of mTORC1 in the disease pathogenesis.

Despite the demonstrated relevance of mTORC1 signaling, there is less known about the molecular mechanisms by which mTORC1 alters cortical development. Addressing this question is complicated by the wide range of cellular processes regulated by mTORC1 through independent downstream targets. Among these regulated processes are autophagy, lysosomal function, lipid synthesis, and, one of the best-studied functions, cap-dependent translation (11). Because current drugs that suppress mTORC1 activity can have serious side effects (12, 13) and do not fully block some of mTORC1's functions (14), a more specific understanding of how mTORC1 contributes to cortical mislamination could yield better targets for treatment.

This study therefore aimed to more closely characterize the cytoarchitectural aberrations generated by hyperactive mTORC1 and to examine the contribution of translational regulation to these cortical malformations. Using in utero electroporation, we generated and characterized focal mislamination and morphological changes driven by mTORC1 signaling. We first examined the contribution of radial glia to mislamination and the molecular identity of the ectopic neurons. We then asked whether up-regulation of cap-dependent translation through eukaryotic initiation factor 4E-binding proteins (4E-BPs) is both necessary for mTORC1-induced misplacement and sufficient to cause ectopic neurons. Our data show that, despite the many other cellular functions regulated by mTORC1, up-regulation of cap-dependent translation through 4E-BPs is both necessary and sufficient for misplacement of cortical projection neurons.

Results

Increasing mTORC1 Activity Results in Ectopic Neuronal Placement. To manipulate mTORC1 activity, we used a plasmid expressing a constitutively active form of Rheb (Rheb S16H or Rheb^{CA}) (15), the canonical activator of mTORC1 (16–18). A mutant, rather than wild type, Rheb was used to better mimic the persistent, dysregulated activation of mTORC1 in the disease state. The construct was introduced into neural progenitors in the developing anterior cingulate cortex (ACC) via in utero electroporation of mouse embryos on embryonic day (E) 15.5 to target layer 2/3 neurons (Fig. 1*A*). As controls, littermates were electroporated with a blue fluorescent protein (BFP)-expressing plasmid. In both conditions, a green fluorescent protein (GFP)-expressing reporter was coelectroporated to visualize the targeted cells. Rheb^{CA} expression was evidenced by an increase in Rheb immunofluorescence (IF) in electroporated cells relative to unelectroporated cells in the contralateral hemisphere at postnatal day (P) 7 and P28 (Fig. S1*A*).

To validate that Rheb^{CA} increased mTORC1 signaling, we examined coronal sections from P21–28 mice for IF of phosphorylated

Significance

Increased mammalian target of rapamycin complex 1 (mTORC1) signaling is associated with many neurological and neurodevelopmental disorders, ranging from epilepsy to autism, that feature developmental defects in the organization of the cortex. Despite the fact that much research has focused on mTORC1-related disorders, the downstream effectors that produce these developmental defects are not well understood. To begin filling that void, this study looked at the role of one of the many cellular processes regulated by mTORC1, cap-dependent translation. Surprisingly, normalizing signaling through only one of mTORC1's targets [eukaryotic initiation factor 4E-binding proteins (4E-BPs)] was able to block ectopic placement of cortical neurons, and mimicking mTORC1 signaling through 4E-BP alone was sufficient to induce neuron misplacement.

Author contributions: T.V.L. and A.B. designed research; T.V.L., L.H., and T.K. performed research; T.V.L., L.H., T.K., and T.J.M. analyzed data; and T.V.L. and A.B. wrote the paper.

The authors declare no conflict of interest.

This article is a PNAS Direct Submission.

[1]To whom correspondence should be addressed. Email: angelique.bordey@yale.edu.

This article contains supporting information online at www.pnas.org/lookup/suppl/doi:10.1073/pnas.1605740113/-/DCSupplemental.

www.pnas.org/cgi/doi/10.1073/pnas.1605740113

Downloaded at Palestinian Territory, occupied on December 15, 2021

www.manaraa.com

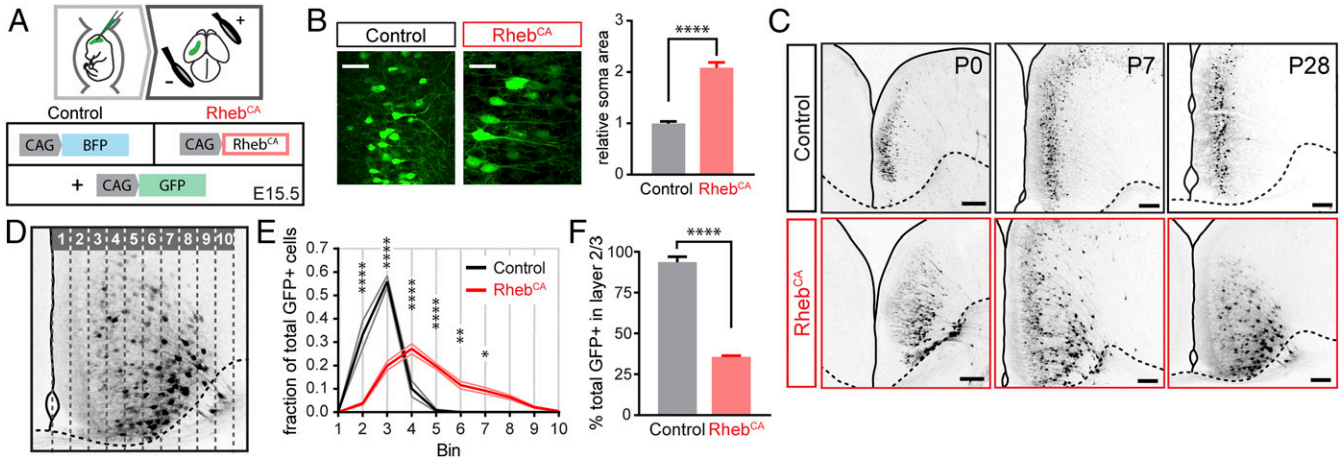

Fig. 1. Increasing mTORC1 activity leads to ectopic neuron placement. (*A*) Schematic of in utero electroporation and constructs used. (*B*) Images of layer 2/3 GFP$^+$ cells in coronal sections from P28 control and Rheb^{CA}-electroporated mice and quantification of soma areas. (Scale bars: 50 μm.) Areas were normalized to control soma area ($n = 25$ cells, 3 mice per condition, *t* test). (*C*) Images of GFP$^+$ cells in ACC from control and Rheb^{CA} electroporated mice at P0, P7, and P28. (Scale bars: 150 μm.) (*D*) Schematic of binning system used to quantify cell distribution. (*E*) Rheb^{CA}-electroporated neurons were more widely distributed relative to controls [$n = 3$ or 4 mice per condition, repeated-measures (RM) two-way ANOVA, Bonferroni post hoc]. (*F*) Quantification of the percent of electroporated neurons that integrate into layer 2/3 ($n = 3$ mice per condition, *t* test). *$P < 0.05$; **$P < 0.005$; ****$P < 0.0001$. All data are presented as mean ± SEM.

S6 (pS6; Ser-240/244), a downstream target of mTORC1 signaling. A 2.3-fold increase in pS6 IF was observed in Rheb^{CA}-electroporated neurons relative to unelectroporated neurons from the contralateral side of the same section (Fig. S1*B*). This increase was not seen in the control condition. We also attempted to analyze p4E-BP1/2 IF, but no signal was detected in the cortex despite staining in the adult neurogenic zone (Fig. S1*C*). However, Rheb^{CA} increased p4E-BP1 (Thr-37/46) levels 2.2-fold in vitro (Fig. S1*D*). Other pathways known to be regulated by mTORC1 signaling were also altered by Rheb^{CA}. Autophagy was decreased at both P7 and P21–28 as evidenced by increased IF for p62, whose levels are negatively regulated by autophagy (19) (Fig. S2). Staining using a KDEL-peptide antibody, which recognizes endoplasmic reticulum (ER) stress markers Grp78, Grp94, and PDI (20), indicated elevated ER stress at both time points (Fig. S3). Finally, we examined soma size because increased mTORC1 activity causes cellular hypertrophy (6, 21–23). As expected, a 2.1-fold increase in soma area was observed in Rheb^{CA}-electroporated cells relative to controls (Fig. 1*B*).

Consistent with other animal models with focal mTORC1 hyperactivation (3–7), Rheb^{CA} produced a striking mislamination effect. This effect was visible from P0 to P28 (Fig. 1*C*). The distribution of neurons was analyzed by dividing the cortex into 10 bins running parallel to the midline from pia to white matter (Fig. 1*D*) and quantifying the proportion of total GFP-positive (GFP$^+$) cells found in each bin. Analysis of tissue from P21–28 mice revealed a significant change in the distribution of the neurons across the cortex in the Rheb^{CA} condition relative to control (Fig. 1*E*). We also found that that only 35% of GFP$^+$ neurons in the Rheb^{CA} condition reached layer 2/3 (delineated by Cux1 or Er81 staining), compared with 93% in controls (Fig. 1*F*).

mTORC1 Signaling Causes Mislamination Independently of Radial Glia. During cortical development, newborn neurons migrate along radial glia processes to their final positions in the cortex (24). Therefore, the Rheb^{CA} mislamination phenotype could be caused by altered mTORC1 signaling in the radial glia (i.e., the scaffolding) rather than in the neurons themselves. To dissociate the contribution of radial glia, we used Rheb^{CA} packaged in a conditional vector (pCALNL-Rheb^{CA}) and coelectroporated it with a plasmid expressing Cre under the *Dcx* promoter (*Dcx*-Cre) (Fig. 2*A*). As a control, the same conditional vector encoding dsRed2 (pCALNL-dsRed) was used. In both conditions, pCALNL-GFP was coelectroporated as a reporter. Because DCX is present in immature migrating neurons, but not in radial glia (25, 26), our conditional constructs should have only begun expressing in the migrating neurons (Fig. 2*B*). As expected, at E18, conditional GFP was expressed outside of the ventricular zone where the radial glia reside (Fig. S4). Analysis at P7 showed that conditional Rheb^{CA}

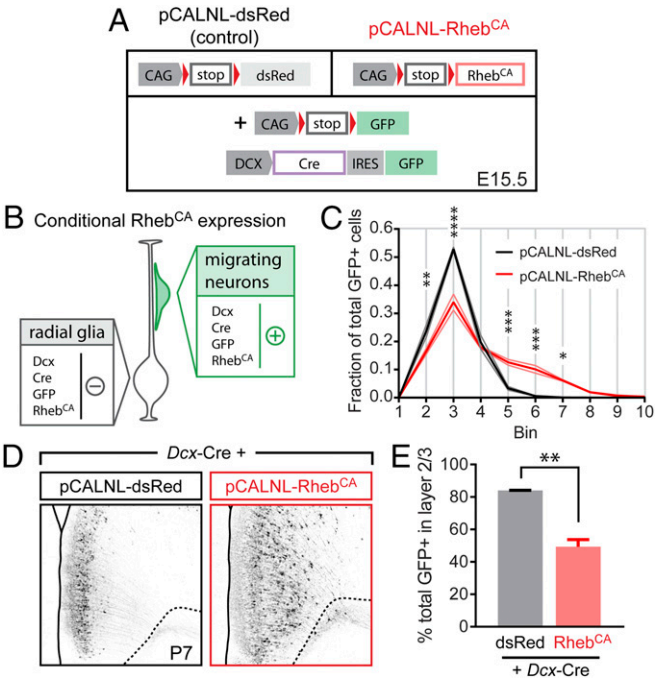

Fig. 2. Rheb^{CA} expression causes mislamination independent of radial glia. (*A*) Summary of constructs used. (*B*) Schematic of conditional plasmid expression in the radial glia and migrating neurons. (*C*) Cells expressing conditional Rheb^{CA} are more widely distributed than control electroporated cells ($n = 3$ mice per condition, RM two-way ANOVA, Bonferroni post hoc). (*D*) Images of GFP$^+$ cells in the ACC of P7 control and Rheb^{CA}-electroporated mice. (*E*) Quantification of the percent of electroporated neurons that integrate into layer 2/3 ($n = 3$ mice per condition, *t* test). *$P < 0.05$; **$P < 0.01$; ***$P < 0.001$; ****$P < 0.0001$. All data are presented as mean ± SEM.

Downloaded at Palestinian Territory, occupied on December 15, 2021
www.manaraa.com

expression in migrating neurons resulted in a significant change in lamination, with 50% of cells failing to reach layer 2/3 (Fig. 2 *C–E*), indicating that Rheb^{CA} expression in the migrating neurons alone is sufficient to induce ectopic integration.

Ectopic Neurons Acquire a Deep-Layer Molecular Identity. Because the majority of Rheb^{CA}-electroporated neurons integrated outside of the expected cortical layer, IF for molecular markers was used to examine changes in the laminar and subtype identities of the ectopic neurons (markers summarized in Fig. 3*A*). To assess laminar identity, we analyzed Cux1 expression, which is restricted to callosal projection neurons of layer 2/3 in the ACC (27). We expected that, if the ectopic neurons retained an upper-layer identity, Cux1 expression would be consistent between neurons found in layer 2/3 and those ectopically integrated in deep layers. In both control and Rheb^{CA} conditions, ∼66% of electroporated neurons in layer 2/3 were Cux1^{+} (64% control, 68% Rheb^{CA}). However, only 26% of Rheb^{CA}-electroporated ectopic neurons in layers 5 and 6 expressed Cux1 (Fig. 3 *B* and *C*). These data suggested a change in identity for the misplaced neurons. To verify that this was the case, we immunostained for Er81, a layer 5 marker (28). Consistent with a change in layer identity, 14% of ectopic cells in layer 5 were Er81^{+} (13.8 ± 2.2%, $n = 4$ mice; Fig. 3*D*).

We next examined markers of projection subtypes. Whereas layer 2/3 projection neurons are callosally projecting, the deep layers contain both callosal and subcortical projection neurons. Subtype identities were therefore examined by using Satb2 [expressed in callosal projection neurons, layers 2–6 (29)], Ctip2 [subcortical projection neurons, layers 5–6 (30)], and Foxp2 [subcortical projection neurons, layer 6 (31)] (Fig. 3*A*). Nearly all GFP^{+} neurons in both control and Rheb^{CA} conditions were positive for Satb2 (control: 98.4 ± 0.5%, Rheb^{CA}: 98.9 ± 0.6%, $n = 3$ mice per condition; Fig. 3*E* and Fig. S5). No ectopic neurons stained for Ctip2 or Foxp2 ($n = 3$ mice; Fig. 3 *F* and *G*), and there were no changes in the expression patterns of these markers. Together, these findings suggest that a subset of ectopic neurons acquire a deep layer identity (Er81^{+}), but all ectopic neurons retain a callosal projection neuron subtype.

Normalizing Cap-Dependent Translation Through 4E-BPs Prevents Ectopic Neurons and Decreases Dendritic Hypertrophy, but Does Not Block Spine Defects. To identify a mechanism for the effects of overactive mTORC1 signaling on cortical aberrations, we explored whether normalizing one of mTORC1's best described functions—regulation of cap-dependent translation—would block the mislamination caused by Rheb^{CA} signaling. Active mTORC1 inhibits 4E-BPs, thereby disinhibiting eIF4E and leading to increased cap-dependent translation. Therefore, to normalize translation, we coelectroporated a constitutively active mutant of 4E-BP1 (4EBP1 F113A or 4EBP1^{CA}) with Rheb^{CA} (Fig. 4*A*). Because this mutant resists phosphorylation by mTORC1 (32, 33), it constitutively binds eIF4E, inhibiting translation and miming the function of all endogenous 4E-BPs. In the control condition, a BFP-expressing plasmid was coelectroporated with Rheb^{CA}.

To test whether our constructs normalized cap-dependent translation, we used a dual luciferase plasmid in which *Renilla* luciferase expression is driven by cap-dependent translation, whereas firefly luciferase expression is mediated by an internal ribosomal entry site, providing an internal control (34). The 4EBP1^{CA} alone inhibited cap-dependent translation by 63% (Fig. S6*A*). Coelectroporating 4EBP1^{CA} with Rheb^{CA} resulted in 4E-BP1 immunostaining (Fig. S6*B*) and normalized cap-dependent translation (Fig. 4*B*), but did not alter the Rheb^{CA}-induced increase in pS6 (Fig. S6*C*). We also found that the increased p62 and KDEL IF caused by Rheb^{CA} was significantly decreased by coexpression of 4EBP1^{CA} at P7 for p62 and at both P7 and P21–28 for KDEL (Figs. S2 and S3). Most importantly, analysis at P7 revealed that 4EBP1^{CA} coelectroporation largely restored neuronal distribution (Fig. 4 *C–E*), with 82.5% of electroporated neurons integrating into layer 2/3 (Fig. 4*C*). These data show that increased cap-dependent translation is necessary for Rheb^{CA} to induce misplacement of cortical pyramidal neurons.

We also examined whether normalizing mTORC1 signaling through another well-characterized target, S6 kinases (S6Ks), could prevent ectopic neurons. A construct expressing an shRNA against both S6K1 and S6K2 (shS6K1/2, previously used by our laboratory to normalize Rheb^{CA} effects on axon length [35]) was coelectroporated with Rheb^{CA}; an empty vector was coelectroporated as a control (Fig. S7*A*). We saw no effect of S6K1/2 knockdown on the misplacement induced by Rheb^{CA} (Fig. S7 *B–D*). This result is in agreement with a previous study that also found that S6K1/2 knockdown was not sufficient to block mTORC1-induced neuronal misplacement (6).

mTORC1 is known to regulate many aspects of neuronal morphology, including soma size (e.g., Fig. 1*B*), dendrite complexity, and spine density, although data on spine regulation are conflicting (9, 22, 23, 36–39). We therefore asked whether normalizing signaling through 4E-BP1 blocked Rheb^{CA}-induced morphological changes. Coelectroporation of 4EBP1^{CA} with

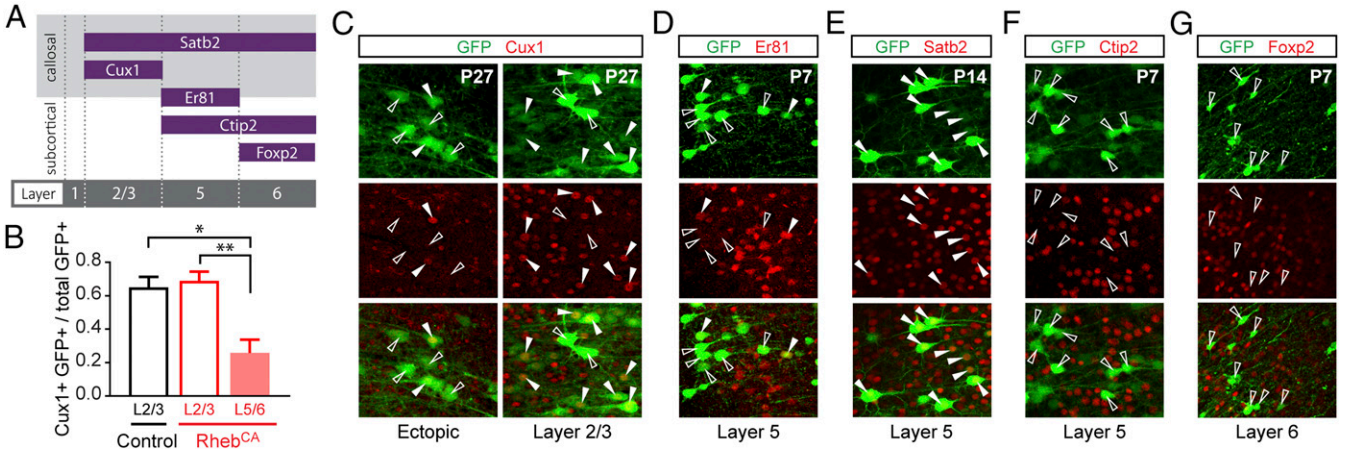

Fig. 3. A subset of ectopic neurons change laminar identity but retain callosal projection subtype. (*A*) Summary of molecular markers used with their layer and subtype restrictions. (*B*) Proportion of GFP^{+} neurons expressing Cux1 in the indicated layers ($n = 4$ mice per condition, one-way ANOVA, Tukey post hoc). *$P < 0.05$; **$P < 0.01$. (*C–G*) Representative images of IF for Rheb^{CA}-electroporated neurons (GFP; green) and the following markers (red): Cux1 (*C*), Er81 (*D*), Satb2 (*E*), Ctip2 (*F*), and Foxp2 (*G*). Filled and open arrowheads represent GFP^{+} neurons positive and negative, respectively, for the marker. (Magnification: 20×.) All data are presented as mean ± SEM.

Downloaded at Palestinian Territory, occupied on December 15, 2021
www.manaraa.com

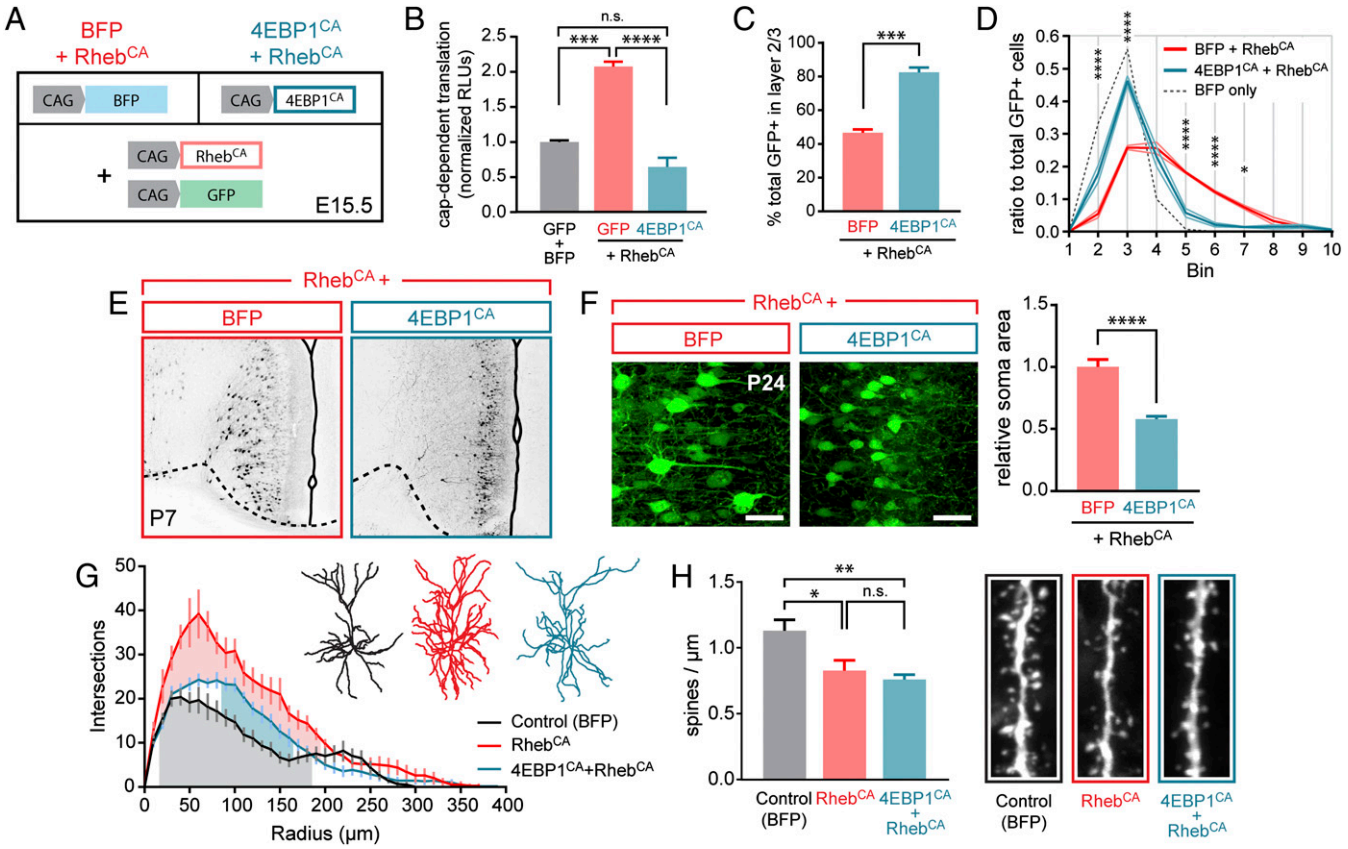

Fig. 4. Normalizing cap-dependent translation prevents neuronal misplacement and some morphological changes induced by hyperactive mTORC1. (*A*) Summary of constructs used. (*B*) Cap-dependent translation as measured by a dual luciferase reporter in Neuro2a cells ($n = 3$ replicates per condition, one-way ANOVA, Tukey post hoc). RLU, relative light units. (*C*) Percent of electroporated cells integrating in layer 2/3 is largely restored in the 4EBP1^{CA}+Rheb^{CA} condition ($n = 3$ mice per condition, t test). (*D*) Distribution of GFP$^+$ neurons in the ACC. BFP-only condition is shown for comparison but is not used in statistical analysis ($n = 3$ mice per condition, RM two-way ANOVA, Bonferroni post hoc). (*E*) Images of GFP$^+$ neurons in coronal sections from P7 mice in BFP+Rheb^{CA} and 4EBP1^{CA}+Rheb^{CA} conditions. (*F*) Images of layer 2/3 GFP$^+$ cells from BFP+Rheb^{CA} and 4EBP1^{CA}+Rheb^{CA} electroporated mice at P24 and soma area quantification ($n = 37$–40 cells, three mice per condition, t test). (Scale bars: 40 μm.) (*G*) Sholl analysis and representative traces of dendrites ($n = 5$–7 cells, three or four mice per condition, RM two-way ANOVA, Bonferroni post hoc). Shaded areas indicate radii where $P < 0.05$. Red shading indicates Rheb^{CA} vs. 4EBP1^{CA}+Rheb^{CA} comparison; blue shading, 4EBP1^{CA}+Rheb^{CA} vs. BFP; gray shading, Rheb^{CA} vs. BFP. (*H*) Spine density quantification and images of basal dendrites in control, Rheb^{CA}, and 4EBP1^{CA}+ Rheb^{CA} neurons ($n = 9$–13 branches, three mice per condition, one-way ANOVA, Tukey post hoc). (Magnification: *H*, 100×.) *$P < 0.05$; ***$P < 0.001$; ****$P < 0.0001$. n.s., not significant. All data are presented as mean ± SEM.

Rheb^{CA} reduced the hypertrophic soma phenotype relative to BFP+Rheb^{CA} (Fig. 4*F*). Dendrite complexity was increased by Rheb^{CA} as measured by Sholl analysis, and 4EBP1^{CA}+Rheb^{CA} significantly reduced, but did not completely block this effect (Fig. 4*G*). Finally, we found that activating mTORC1 led to a significant decrease in spine density in basal dendrites (Fig. 4*H*). Coelectroporation of 4EBP1^{CA} with Rheb^{CA} had no effect on this spine density phenotype. These data suggest that increased translation is not required for the Rheb^{CA}-driven spine defect, but contributes to soma and dendrite hypertrophy.

To ensure that neurons remained functional despite knocking down cap-dependent translation, we performed patch-clamp recordings of layer 2/3 neurons in control (BFP), Rheb^{CA}, and Rheb^{CA}+4EBP1^{CA} conditions. The resting membrane potential of the Rheb^{CA}-electroporated neurons was significantly more depolarized than that of control neurons (control, −75 mV; Rheb^{CA}, −67 mV) but was restored to control levels with 4EBP1^{CA} coexpression (−77 mV) (Fig. S8*A*). Transfected neurons from all conditions showed no gross differences in their depolarization-induced firing properties (Fig. S8*B*). Although neurons in all conditions received synaptic inputs, Rheb^{CA} decreased the frequency of spontaneous excitatory postsynaptic currents (sEPSCs), and coexpression of 4EBP1^{CA} normalized this decrease (Fig. S8*C*). Thus, limiting cap-dependent translation in neurons with hyperactive mTORC1 did not impair physiological function and restored Rheb^{CA}-induced changes to resting membrane potential and sEPSC frequency.

Knockdown of 4E-BP2 Is Sufficient to Induce Ectopic Placement Independently of mTORC1. Because blocking the Rheb^{CA}-induced increase in cap-dependent translation prevented ectopic placement, we asked whether increasing cap-dependent translation independently of mTORC1 is sufficient to recapitulate the misplacement seen with Rheb^{CA}. To address this question, we knocked down 4E-BP2, the predominant 4E-BP in the brain (40), with an shRNA-expressing plasmid (sh4EBP2) (Fig. 5*A*). An empty vector was used as a control. sh4EBP2 increased cap-dependent translation by 65% at P7 (Fig. 5*B*) and knocked down protein levels of 4E-BP2 by ∼84% in vitro relative to controls (Fig. 5*C*). The effect of sh4EBP2 on translation was not effective by P21–28 (Fig. S9*A*). This knockdown did not result in a compensatory increase in 4E-BP1 protein levels (Fig. S9 *B* and *C*). No change in ER stress markers was observed (Fig. S3 *C* and *D*), although there was a very small, significant increase in p62 IF (Fig. S2 *C* and *D*).

Electroporation was performed 1 d earlier than previous experiments (E14.5) to account for the longer time needed to achieve

Downloaded at Palestinian Territory, occupied on December 15, 2021
www.manaraa.com

the functional effect of an shRNA relative to an overexpressed gene. Electroporating earlier also resulted in labeling of more superficial layer 5 neurons relative to electroporation at E15.5. Knockdown of 4E-BP2 was sufficient to induce ectopic integration of neurons (Fig. 5 *D–F*), although the deficit was milder than that seen with Rheb^{CA}. Whereas 74% of control electroporated neurons integrated into layer 2/3, only 64% of neurons with sh4EBP2 did the same (Fig. 5*E*). Quantification of electroporated cells that reside within the deeper half of the cortex showed that only 2% of control cells were found in the deep half, compared with 14% of those with sh4EBP2 (Fig. 5*F*). We therefore conclude that enhancing cap-dependent translation through knockdown of 4E-BP2 is sufficient to induce ectopic placement of neurons.

Discussion

Our data show that the misplacement of cortical neurons induced by mTORC1 signaling (*i*) does not require aberrant mTORC1 signaling in radial glia; (*ii*) involves changes in laminar, but not projection subtype identity of ectopic neurons; and (*iii*) requires up-regulation of cap-dependent translation through 4E-BPs. Finally, disinhibiting translation through knockdown of 4E-BP2 alone is sufficient to induce ectopic placement of neurons.

By analyzing Er81—a marker specific for laminar, but not projection subtype identity (28)—we show that many ectopic neurons can acquire the identity of the layer into which they integrate. That only a subset of our ectopic neurons express Er81 is not surprising, given that Er81 is typically only expressed in 34% of layer 5 callosal projection neurons (41). Analysis of subtype markers Satb2, Ctip2, and Foxp2 also showed that ectopic neurons do not switch projection subtype, which is in agreement with a previous study examining Ctip2 and Tbr1 after in utero electroporation of a *Tsc2* shRNA (5).

Normalization of cap-dependent translation using coexpression of 4EBP1^{CA} prevented the mislamination induced by hyperactive mTORC1. Furthermore, 4E-BP2 knockdown alone was sufficient to cause ectopic integration. These data add to findings by others that demonstrate that manipulating 4E-BP–eIF4E can generate disordered neuronal phenotypes (40, 42–46). The milder phenotype observed with sh4EBP2 relative to Rheb^{CA} was likely not because of 4E-BP1 compensation based on our data, but could be due to a number of factors: (*i*) the increase in cap-dependent translation by sh4EBP2 was smaller than that with Rheb^{CA} expression; (*ii*) differences in timing due to the delayed functional effects of shRNAs; and (*iii*) although increased translation is necessary for mislamination, other branches of mTORC1 signaling may contribute to the Rheb^{CA} phenotype.

Interestingly, our IF analyses showed that 4E-BPs can regulate the Rheb^{CA}-driven changes to autophagy and ER stress at P7. With respect to autophagy, this finding is unexpected because mTORC1 can regulate this pathway independently of 4E-BPs (47, 48). Our data suggest that mTORC1 signaling can also indirectly alter autophagy through regulation of translation. The extent to which translation-regulated changes to autophagy and ER stress signaling contributes, if at all, to mTORC1-induced mislamination is yet to be determined. The 4E-BP2 knockdown did not change KDEL staining intensity, which may indicate that elevated ER stress is not necessary for ectopic neuron placement. However, it may also be that immunostaining is not sensitive enough to detect moderate changes in ER stress signaling.

In addition to causing mislamination, we found that Rheb^{CA} depolarizes the resting membrane potential and decreases sEPSC frequency, while increasing soma size and dendritic complexity and decreasing spine density. Additional studies would be required to examine whether changes in ion channel expression in addition to morphological defects may account for the biophysical alterations. Although mTORC1-induced somatic and dendritic overgrowth is well established, past reports on the effects on membrane potential, spine density, and synaptic event frequencies are highly varied. The diversity of outcomes is likely due at least in part to differences in the model systems used, which vary by cell type, experimental preparation (e.g., culture vs. acute slice), and molecular target (e.g., Pten or Tsc1/2). Normalizing signaling through 4E-BPs ameliorated most of our observed phenotypes, with spine density as a notable exception. Our spine data complement studies reporting that some TSC–Rheb effects on spines are dependent on autophagy (38) or are potentially mTORC1-independent (23, 39).

The necessity of mTORC1 signaling through 4E-BPs for disordered neuron integration emphasizes the importance of cap-dependent translation on cortical development, with dysregulation leading to mislamination and neuronal dysmorphogenesis. Our findings are important with respect to many neurological disorders that exhibit dysregulated mTORC1 activity and translation, such as fragile X syndrome, PTEN-related syndromes, and tuberous sclerosis complex. Of the many effectors downstream of mTORC1, we identified 4E-BPs as a molecular target that can restore many aspects of normal cortical circuitry. Considering that rapamycin does not fully block mTORC1 signaling through 4E-BPs in vitro (14), our report that normalizing signaling through 4E-BPs, but not S6Ks, prevents Rheb^{CA}-induced mislamination seems to conflict with studies showing that rapamycin can rescue many phenotypes, including mislamination, in TSC models (5, 7, 49). However, the effects of rapamycin on translation and 4E-BP signaling after chronic administration in vivo are not well studied, particularly in the brain. Interestingly, one study showed substantial repression of total and p4E-BP1 in the cortex with chronic rapamycin injections (6), opening the possibility that 4E-BP repression may contribute to the benefits of rapamycin

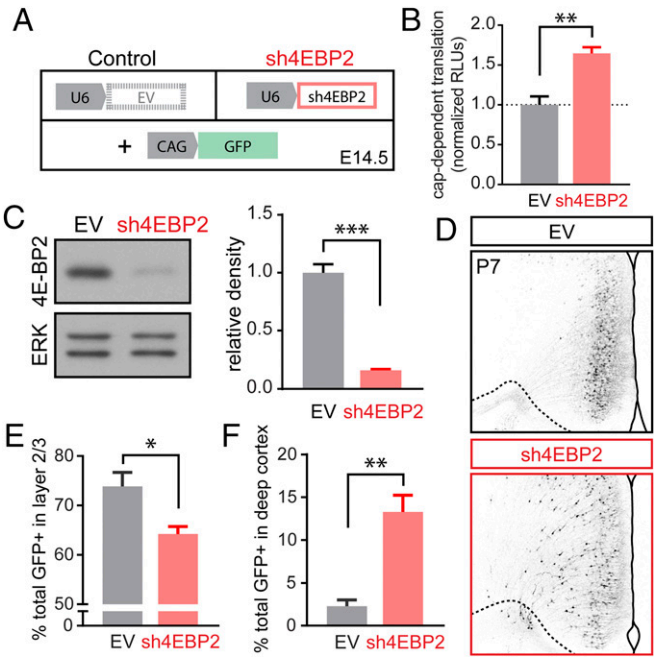

Fig. 5. Knockdown of 4E-BP2 is sufficient to induce ectopic neuron placement. (*A*) Summary of constructs used. (*B*) Cap-dependent translation as measured by a dual luciferase reporter construct in electroporated ACC ($n = 3$ mice/condition). (*C*) Western blots and quantification of 4E-BP2 in vitro. The 4E-BP2 was normalized to ERK1/2 (Neuro2a; $n = 3$ replicates per condition). (*D*) Representative images from coronal sections of P7 mice. (*E*) Percent of electroporated cells integrating into layer 2/3 is decreased in sh4EBP2 condition vs. control ($n = 3$ per condition). (*F*) More electroporated cells integrate into the deeper half of the cortex in sh4EBP2 condition relative to control ($n = 3$ mice per condition). All analyses: *t* test. $^*P < 0.05$; $^{**}P < 0.01$; $^{***}P < 0.001$. All data are presented as mean ± SEM.

Downloaded at Palestinian Territory, occupied on December 15, 2021
www.manaraa.com

treatment. Given that rapamycin affects many processes and can cause serious side effects, understanding which effectors of mTORC1 signaling contribute to specific phenotypes could inform and improve options for treatment. Our data point to 4E-BPs and their downstream targets as promising candidates for further study and therapeutic targeting.

Materials and Methods

All procedures and protocols were approved by the Yale University Institutional Animal Care and Use Committee. All mice used were timed pregnant CD-1 mice (Charles River) and their pups. Detailed methods can be found in *SI Materials and Methods* and Table S1.

ACKNOWLEDGMENTS. We thank Drs. Hanada and Maehama (National Institute of Infectious Diseases) for the Rheb^{CA} vector; Dr. Mueller (Scripps) for the *Dcx*-Cre construct; Dr. Blenis (Weill Cornell) for the luciferase reporter; and Drs. Caplan and Kim (Yale University) for use of their luminometers. This work was supported by NIH Grant R01 NS086329, a McKnight Endowment Fund for Neuroscience award (to A.B.), the Pfizer Patricia Goldman-Rakic Fellowship (to T.V.L.), and NIH Grant GM007324 (to T.J.M.).

1. Crino PB (2011) mTOR: A pathogenic signaling pathway in developmental brain malformations. *Trends Mol Med* 17(12):734–742.
2. Leventer RJ, et al. (1999) Clinical and imaging features of cortical malformations in childhood. *Neurology* 53(4):715–722.
3. Orlova KA, et al. (2010) STRADalpha deficiency results in aberrant mTORC1 signaling during corticogenesis in humans and mice. *J Clin Invest* 120(5):1591–1602.
4. Feliciano DM, Su T, Lopez J, Platel J-C, Bordey A (2011) Single-cell Tsc1 knockout during corticogenesis generates tuber-like lesions and reduces seizure threshold in mice. *J Clin Invest* 121(4):1596–1607.
5. Tsai V, et al. (2014) Fetal brain mTOR signaling activation in tuberous sclerosis complex. *Cereb Cortex* 24(2):315–327.
6. Kassai H, et al. (2014) Selective activation of mTORC1 signaling recapitulates microcephaly, tuberous sclerosis, and neurodegenerative diseases. *Cell Reports* 7(5):1626–1639.
7. Moon UY, et al. (2015) Impaired Reelin-Dab1 signaling contributes to neuronal migration deficits of tuberous sclerosis complex. *Cell Reports* 12(6):965–978.
8. Ehninger D, et al. (2008) Reversal of learning deficits in a Tsc2+/- mouse model of tuberous sclerosis. *Nat Med* 14(8):843–848.
9. Meikle L, et al. (2008) Response of a neuronal model of tuberous sclerosis to mammalian target of rapamycin (mTOR) inhibitors: Effects on mTORC1 and Akt signaling lead to improved survival and function. *J Neurosci* 28(21):5422–5432.
10. Parker WE, et al. (2013) Rapamycin prevents seizures after depletion of STRADA in a rare neurodevelopmental disorder. *Sci Transl Med* 5(182):182ra53.
11. Laplante M, Sabatini DM (2012) mTOR signaling in growth control and disease. *Cell* 149(2):274–293.
12. Tsai PT, et al. (2013) Prenatal rapamycin results in early and late behavioral abnormalities in wildtype C57BL/6 mice. *Behav Genet* 43(1):51–59.
13. Sadowski K, Kotulska K, Jóźwiak S (2016) Management of side effects of mTOR inhibitors in tuberous sclerosis patients. *Pharmacol Rep* 68(3):536–542.
14. Kang SA, et al. (2013) mTORC1 phosphorylation sites encode their sensitivity to starvation and rapamycin. *Science* 341(6144):1236566.
15. Yan L, et al. (2006) Hyperactivation of mammalian target of rapamycin (mTOR) signaling by a gain-of-function mutant of the Rheb GTPase. *J Biol Chem* 281(29):19793–19797.
16. Garami A, et al. (2003) Insulin activation of Rheb, a mediator of mTOR/S6K/4E-BP signaling, is inhibited by TSC1 and 2. *Mol Cell* 11(6):1457–1466.
17. Inoki K, Li Y, Xu T, Guan K-L (2003) Rheb GTPase is a direct target of TSC2 GAP activity and regulates mTOR signaling. *Genes Dev* 17(15):1829–1834.
18. Tee AR, Manning BD, Roux PP, Cantley LC, Blenis J (2003) Tuberous sclerosis complex gene products, Tuberin and Hamartin, control mTOR signaling by acting as a GTPase-activating protein complex toward Rheb. *Curr Biol* 13(15):1259–1268.
19. Bjørkøy G, et al. (2005) p62/SQSTM1 forms protein aggregates degraded by autophagy and has a protective effect on huntingtin-induced cell death. *J Cell Biol* 171(4):603–614.
20. Lee AS (2001) The glucose-regulated proteins: Stress induction and clinical applications. *Trends Biochem Sci* 26(8):504–510.
21. Kwon C-H, Zhu X, Zhang J, Baker SJ (2003) mTor is required for hypertrophy of Pten-deficient neuronal soma in vivo. *Proc Natl Acad Sci USA* 100(22):12923–12928.
22. Kumar V, Zhang M-X, Swank MW, Kunz J, Wu G-Y (2005) Regulation of dendritic morphogenesis by Ras-PI3K-Akt-mTOR and Ras-MAPK signaling pathways. *J Neurosci* 25(49):11288–11299.
23. Tavazoie SF, Alvarez VA, Ridenour DA, Kwiatkowski DJ, Sabatini BL (2005) Regulation of neuronal morphology and function by the tumor suppressors Tsc1 and Tsc2. *Nat Neurosci* 8(12):1727–1734.
24. Rakic P (1972) Mode of cell migration to the superficial layers of fetal monkey neocortex. *J Comp Neurol* 145(1):61–83.
25. Francis F, et al. (1999) Doublecortin is a developmentally regulated, microtubule-associated protein expressed in migrating and differentiating neurons. *Neuron* 23(2):247–256.
26. Gleeson JG, Lin PT, Flanagan LA, Walsh CA (1999) Doublecortin is a microtubule-associated protein and is expressed widely by migrating neurons. *Neuron* 23(2):257–271.
27. Nieto M, et al. (2004) Expression of Cux-1 and Cux-2 in the subventricular zone and upper layers II-IV of the cerebral cortex. *J Comp Neurol* 479(2):168–180.
28. Hevner RF, et al. (2003) Beyond laminar fate: Toward a molecular classification of cortical projection/pyramidal neurons. *Dev Neurosci* 25(2-4):139–151.
29. Alcamo EA, et al. (2008) Satb2 regulates callosal projection neuron identity in the developing cerebral cortex. *Neuron* 57(3):364–377.
30. Arlotta P, et al. (2005) Neuronal subtype-specific genes that control corticospinal motor neuron development in vivo. *Neuron* 45(2):207–221.
31. Ferland RJ, Cherry TJ, Preware PO, Morrisey EE, Walsh CA (2003) Characterization of Foxp2 and Foxp1 mRNA and protein in the developing and mature brain. *J Comp Neurol* 460(2):266–279.
32. Choi KM, McMahon LP, Lawrence JC, Jr (2003) Two motifs in the translational repressor PHAS-I required for efficient phosphorylation by mammalian target of rapamycin and for recognition by raptor. *J Biol Chem* 278(22):19667–19673.
33. Schalm SS, Fingar DC, Sabatini DM, Blenis J (2003) TOS motif-mediated raptor binding regulates 4E-BP1 multisite phosphorylation and function. *Curr Biol* 13(10):797–806.
34. Li S, et al. (2002) Translational control of cell fate: Availability of phosphorylation sites on translational repressor 4E-BP1 governs its proapoptotic potency. *Mol Cell Biol* 22(8):2853–2861.
35. Gong X, et al. (2015) Activating the translational repressor 4E-BP or reducing S6K-GSK3β activity prevents accelerated axon growth induced by hyperactive mTOR in vivo. *Hum Mol Genet* 24(20):5746–5758.
36. Jaworski J, Spangler S, Seeburg DP, Hoogenraad CC, Sheng M (2005) Control of dendritic arborization by the phosphoinositide-3′-kinase-Akt-mammalian target of rapamycin pathway. *J Neurosci* 25(49):11300–11312.
37. Bateup HS, Takasaki KT, Saulnier JL, Denefrio CL, Sabatini BL (2011) Loss of Tsc1 in vivo impairs hippocampal mGluR-LTD and increases excitatory synaptic function. *J Neurosci* 31(24):8862–8869.
38. Tang G, et al. (2014) Loss of mTOR-dependent macroautophagy causes autistic-like synaptic pruning deficits. *Neuron* 83(5):1131–1143.
39. Yasuda S, et al. (2014) Activation of Rheb, but not of mTORC1, impairs spine synapse morphogenesis in tuberous sclerosis complex. *Sci Rep* 4:5155.
40. Banko JL, et al. (2005) The translation repressor 4E-BP2 is critical for eIF4F complex formation, synaptic plasticity, and memory in the hippocampus. *J Neurosci* 25(42):9581–9590.
41. Yoneshima H, et al. (2006) Er81 is expressed in a subpopulation of layer 5 neurons in rodent and primate neocortices. *Neuroscience* 137(2):401–412.
42. Banko JL, Hou L, Poulin F, Sonenberg N, Klann E (2006) Regulation of eukaryotic initiation factor 4E by converging signaling pathways during metabotropic glutamate receptor-dependent long-term depression. *J Neurosci* 26(8):2167–2173.
43. Banko JL, et al. (2007) Behavioral alterations in mice lacking the translation repressor 4E-BP2. *Neurobiol Learn Mem* 87(2):248–256.
44. Ran I, et al. (2013) Selective regulation of GluA subunit synthesis and AMPA receptor-mediated synaptic function and plasticity by the translation repressor 4E-BP2 in hippocampal pyramidal cells. *J Neurosci* 33(5):1872–1886.
45. Gkogkas CG, et al. (2013) Autism-related deficits via dysregulated eIF4E-dependent translational control. *Nature* 493(7432):371–377.
46. Santini E, et al. (2013) Exaggerated translation causes synaptic and behavioural aberrations associated with autism. *Nature* 493(7432):411–415.
47. Hosokawa N, et al. (2009) Nutrient-dependent mTORC1 association with the ULK1-Atg13-FIP200 complex required for autophagy. *Mol Biol Cell* 20(7):1981–1991.
48. Jung CH, et al. (2009) ULK-Atg13-FIP200 complexes mediate mTOR signaling to the autophagy machinery. *Mol Biol Cell* 20(7):1992–2003.
49. Ehninger D (2013) From genes to cognition in tuberous sclerosis: Implications for mTOR inhibitor-based treatment approaches. *Neuropharmacology* 68:97–105.
50. Niwa H, Yamamura K, Miyazaki J (1991) Efficient selection for high-expression transfectants with a novel eukaryotic vector. *Gene* 108(2):193–199.
51. Matsuda T, Cepko CL (2004) Electroporation and RNA interference in the rodent retina in vivo and in vitro. *Proc Natl Acad Sci USA* 101(1):16–22.
52. Ventura A, et al. (2004) Cre-lox-regulated conditional RNA interference from transgenes. *Proc Natl Acad Sci USA* 101(28):10380–10385.
53. Rodriguez A, Ehlenberger DB, Dickstein DL, Hof PR, Wearne SL (2008) Automated three-dimensional detection and shape classification of dendritic spines from fluorescence microscopy images. *PLoS One* 3(4):e1997.
54. Choo AY, Yoon S-O, Kim SG, Roux PP, Blenis J (2008) Rapamycin differentially inhibits S6Ks and 4E-BP1 to mediate cell-type-specific repression of mRNA translation. *Proc Natl Acad Sci USA* 105(45):17414–17419.
55. Maehama T, et al. (2008) RalA functions as an indispensable signal mediator for the nutrient-sensing system. *J Biol Chem* 283(50):35053–35059.
56. Bae EJ, et al. (2012) Liver-specific p70 S6 kinase depletion protects against hepatic steatosis and systemic insulin resistance. *J Biol Chem* 287(22):18769–18780.
57. Franco SJ, Martinez-Garay I, Gil-Sanz C, Harkins-Perry SR, Müller U (2011) Reelin regulates cadherin function via Dab1/Rap1 to control neuronal migration and lamination in the neocortex. *Neuron* 69(3):482–497.

Downloaded at Palestinian Territory, occupied on December 15, 2021

www.manaraa.com